Frontiers of Information Technology & Electronic Engineering
www.jzus.zju.edu.cn; engineering.cae.cn; www.springerlink.com
ISSN 2095-9184 (print); ISSN 2095-9230 (online)
E-mail: jzus@zju.edu.cn

An algorithm for trajectory prediction of flight plan based on relative motion between positions*

Yi LIN[†1, 2], Jian-wei ZHANG[1, 2], Hong LIU[†‡1, 2]

[1]*National Key Laboratory of Fundamental Science on Synthetic Vision, Sichuan University, Chengdu 610065, China*

[2]*National Key Laboratory of Air Traffic Control Automation System Technology, Sichuan University, Chengdu 610065, China*

[†]E-mail: Scu_lyi@stu.scu.edu.cn; liuhong@scu.edu.cn

Received Apr. 5, 2017; Revision accepted May 22, 2017; Crosschecked July 8, 2018

Abstract: Traditional methods for plan path prediction have low accuracy and stability. In this paper, we propose a novel approach for plan path prediction based on relative motion between positions (RMBP) by mining historical flight trajectories. A probability statistical model is introduced to model the stochastic factors during the whole flight process. The model object is the sequence of velocity vectors in the three-dimensional Earth space. First, we model the moving trend of aircraft including the speed (constant, acceleration, or deceleration), yaw (left, right, or straight), and pitch (climb, descent, or cruise) using a hidden Markov model (HMM) under the restrictions of aircraft performance parameters. Then, several Gaussian mixture models (GMMs) are used to describe the conditional distribution of each moving trend. Once the models are built, machine learning algorithms are applied to obtain the optimal parameters of the model from the historical training data. After completing the learning process, the velocity vector sequence of the flight is predicted by the proposed model under the Bayesian framework, so that we can use kinematic equations, depending on the moving patterns, to calculate the flight position at every radar acquisition cycle. To obtain higher prediction accuracy, a uniform interpolation method is used to correct the predicted position each second. Finally, a plan trajectory is concatenated by the predicted discrete points. Results of simulations with collected data demonstrate that this approach not only fulfils the goals of traditional methods, such as the prediction of fly-over time and altitude of waypoints along the planned route, but also can be used to plan a complete path for an aircraft with high accuracy. Experiments are conducted to demonstrate the superiority of this approach to some existing methods.

Key words: Velocity vector; Hidden Markov model; Gaussian mixture model; Machine learning; Plan path prediction; Relative motion between positions (RMBP)

https://doi.org/10.1631/FITEE.1700224 **CLC number:** TP391

1 Introduction

Trajectory prediction (TP) for flight is a basic technique used in many applications of air traffic management (ATM) systems, such as traffic flow forecasting, conflict detection, and the dynamic use of airspace units. With the increasing popularity of trajectory based operations (TBOs), trajectory prediction with high accuracy plays a more important role in airspace resource optimization and advanced air traffic flow management (ATFM). It is also an indispensable tool to ensure flight safety, maintain the traffic order, and increase the traffic capacity. It also promotes fuel savings and reduces pollutant gas emissions. With the growth of air traffic, a fixed amount of airspace, serious flight congestion, and delays frequently occur in large air traffic hubs, such as Beijing and Shanghai in China. Thus, trajectory

‡ Corresponding author

* Project supported by the National Natural Science Foundation of China (No. 71573184), the National Key Scientific Instrument and Equipment Development Project (No. 2013YQ490879), and the Special Program of Office of China Air Traffic Control Commission (No. GKG201403004)

ORCID: Yi LIN, http://orcid.org/0000-0002-7194-5023

prediction is highly desired for better planning and use of airspace resources. The Single European Sky Air Traffic Management Research (SESAR) and the Next Generation of Air Transportation System (Next Gen) programs have already recognized the importance of trajectory prediction (Gardi et al., 2013).

There have been many outstanding findings in this field. Early studies focused mainly on kinematics and dynamics models with preset parameters. Chen (2010) divided the whole flight process into three phases, classic climb, cruise, and descent. Then, he constructed and solved the kinematics and dynamics equations with a simplified model in each phase to accomplish trajectory estimation. However, because of the unclear boundaries between adjacent phases, the prediction results showed a large deviation from the ground truth. Zhang et al. (2014) proposed algorithms based on aircraft performance parameters drawn from the base of aircraft data (BADA). However, they did not consider the change of the environment, so they also failed to obtain an accurate prediction. Gardi et al. (2013) also used the recommended dynamics parameters taken from BADA to estimate the flight trajectory. However, the motion patterns of a certain flight cannot be appropriately described by those theoretical parameters. As the mass storage of historical trajectories containing real-time environmental factors came into practice, researchers began to focus on mining historical trajectories. Wandelt and Sun (2015) proposed a trajectory compression algorithm for saving computer storage, providing sufficient training samples for machine learning algorithms. Tang et al. (2015c) introduced a method based on velocity correction to estimate the path taken during aircraft taxiing. Xie and Cheng (2015) presented an algorithm to design the route taken in terminal areas by mining the frequent patterns from historical trajectories in the stored radar data. A prediction algorithm based on the moving parameters mined from historical data was described by Song (2012). Although these methods avoid the deficiency of setting parameters, they are still limited in terms of accuracy because of the flaws inherent in the models. Hamed et al. (2013) proposed a statistical model for aircraft trajectory prediction based on a combination of a kinematic stochastic model and a probabilistic performance model. A hidden Markov model (HMM) is applied to distinguish the flight phases, followed by a kernel density estimation (KDE) to model the kinematic randomness. Tang et al. (2015a) proposed a method to extract the nominal flight profile and revised airway meteorological forecasts to mine the patterns of historical flight. Tang et al. (2015b) presented a prediction method with a clustering algorithm to obtain the moving rules in different periods of flight. The basic ideas in these methods are similar, but the model approaches and model objects are different. An extended application of trajectory prediction was proposed by Li et al. (2015) to achieve more efficient management of general aviation aircraft.

Although historical data has been introduced in the latest methods, the estimation results are still not ideal, because the models do not consider the randomness of the flight condition. Moreover, because of the high maneuverability of aircraft during the climb and descent stages, obtaining an accurate trajectory prediction is really a challenge. Yepes et al. (2007) introduced a hybrid estimation algorithm to overcome this problem by combining the knowledge of air traffic control regulations, the flight plan, and the pilot's intent. Some researchers have managed to apply HMM to trajectory prediction with impressive results. Morzy (2007) introduced a frequent trajectory mining algorithm to predict the location of moving objects, such as cars and pedestrians. Jeung et al. (2007) used HMM to mine trajectory patterns. They obtained trajectory predictions by splitting the whole map into grids of fixed size to avoid the answer-loss problem. Qiao SJ et al. (2015b) improved the accuracy of the model by incorporating self-adaptive learning of parameters in the algorithm. Naseri et al. (2007) used a hybrid hidden Markov model (HHMM) to perform mode detection on collected flight track data. After tuning the discrete and continuous parameters, the level of ascending and descending transition was tested to validate the effectiveness of HHMM. Shanmuganathan (2014) designed a prediction model applying HMM and cluster analysis to estimate the spatial-temporal trajectories of a storm in the southern USA. Ayhan and Samet (2016) described a novel stochastic trajectory prediction approach to estimate the near future situation in given airspace, based on which better decisions and advisories can be made. The focus of their study was to model the real-time weather environment. They considered the airspace

as a 3D grid network, and a weather model was built for each grid with corresponding weather conditions. Finally, HMM was used to predict trajectories by taking environmental uncertainties into account. Lymperopoulos and Lygeros (2010) introduced sequential Monte Carlo methods for multi-aircraft trajectory prediction in ATM. Their method combined information from multiple aircraft at different locations and time instants.

To obtain a more credible trajectory prediction and improve its adaptability in Chinese civil aviation, we present a hybrid stochastic statistical model. Our model combines HMM with Gaussian mixture model (GMM) to predict the flight path before the flight execution by mining the motion patterns from collected historical surveillance data, such as radar and automatic dependency surveillance-broadcasts (ADS-B). The basic idea of our proposed model is that, for a certain flight, flight trajectories executed on different days follow the same moving trend and share the same waypoint sequence. The model assumes that, in every moving trend, motion parameters (dynamic parameters), which constitute three attributes in the velocity vector, namely, speed, yaw, and pitch, follow a learnable distribution. At different time instants and positions, these three parameters have different values, indicating that there is relative motion between different positions. A transition model of the motion state is built using HMM, according to the statistic of relative motion between positions (RMBP). GMMs are used to describe the distributions of moving parameters in different moving trends.

The proposed models contain several parameters that need to be optimized. We learn the optimal model parameters using training samples (collected historical flight track). After the optimal model parameters are found, the motion parameters are accordingly computed. Then, the complete path is calculated by using kinematics equations between adjacent update moments. An individual model is created for each flight with motion trend and degree treated, separately. The motion trend is modeled to predict the velocity change trend, and the degree predicts the motion parameters from GMM. The parameter learning processes of HMM and GMM reflect the frequent patterns of certain flights. Then the most likely motion trend is obtained using the Markov chain Monte Carlo (MCMC) sampling method, and the value of the motion parameters is predicted under Bayesian framework.

Our main contributions are summarized as follows:

1. A hybrid statistical model with double stochastic process involving HMM and GMMs is introduced to model the flight process, taking implicit uncertainties of flight into consideration.

2. We apply HMM to model the moving trend transition with a 3D velocity vector (speed, yaw, and pitch) during flight.

3. GMMs are used to depict the distribution of motion parameters in different moving trends.

4. Machine learning algorithms, such as expectation maximization (EM) and MCMC sampling of the velocity vector, are employed to predict a complete flight path.

2 Related background information

2.1 Historical data

The trajectories of all flights can be collected by the surveillance equipment. At the same time, the cooperative targets send their position, motion parameters, and flight intentions through ADS-B. All the real-time information, such as flight plans, control factors, and trajectories, is eventually fed into the air traffic control system (ATCS). Supposing that the historical trajectories are stored in a centralized or distributed database (Zheng and Zhou, 2012), we can access the trajectories via a robust data bus. Such a trajectory database is organized as shown in Fig. 1.

In Fig. 1, the storage structure of the trajectory data is marked by the unique identifier of the flights, for example, flight-1, flight-2, …, flight-m. The trajectory dataset of a certain flight f_c contains n paths, path-1, path-2, …, path-n, in which each path is collected on different execution days. All the paths are processed by filtering, smoothing, and interpolation (Zheng and Zhou, 2012) before training to keep the same update interval. A collected flight path consists of k discrete points, which are sampled in a time series with sampling intervals of 4 s. In practice, each stored discrete point includes almost 15 attribution items. In this study, only the velocity vectors are considered in modeling and training, and the positions

are used to evaluate the accuracy and stability of the prediction results. The attributions of a trajectory point are expressed in Eq. (1), including longitude, latitude, altitude, horizontal velocity, heading, and vertical velocity:

$$\boldsymbol{p}=[x,y,z,vh,\omega h,vz,\omega z]^{\mathrm{T}}. \tag{1}$$

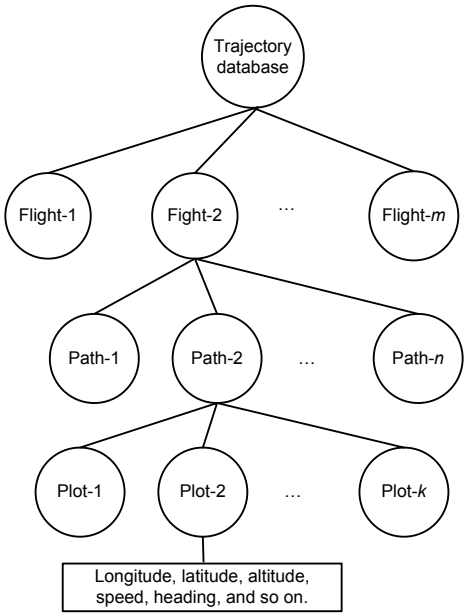

Fig. 1 Structure of the trajectory database

In this study, we predict a complete flight path consisting of discrete points, whose update intervals are the same as those of surveillance equipment. There is a tiny difference between two neighboring positions if the positions are represented by the coordinates of longitude and latitude. Therefore, this would be vanished in the training and prediction process. Based on these considerations, the longitude and latitude measurements in the database are combined into one rectangular coordinate system, whose center is assigned to the origin of multi-radar data fusion, i.e., (102.5, 20.5, 500). To reduce the complexity of modeling, we convert all the velocity related parameters into polar coordinates. Then the velocity vector $[vh, \omega h, vz, \omega z]^{\mathrm{T}}$ is simplified as $[s, \vartheta, \theta]^{\mathrm{T}}$, in which s, ϑ, and θ denote the speed, yaw, and pitch of an aircraft in polar coordinates, respectively.

Except for some irregular conditions, such as returning and alternating, each execution of the same flight in historical data was performed along the same route and over the same key points. The historical routes are proven to be safe and feasible. Environmental factors along the route are also taken into consideration, so the flight process model parameters can be well established by mining the historical trajectory data.

2.2 Hidden Markov model

HMM is a statistical model of a dual stochastic process, in which the state relationships between instants of time series are depicted by the hidden states transition and the probability distribution between the hidden states and observations (Qiao MY et al., 2015; Zahariand and Jaafar, 2015). HMM contains the following parameters:

$$\lambda=\{O,S,\boldsymbol{A},\boldsymbol{B},\pi_0\}, \tag{2}$$

where $O=\{o_1, o_2, \ldots, o_T\}$ is an observation sequence. T is the total length of the time series, which in our work is the number of update cycles. A hidden state set S consists of a finite number of discrete states. There is always a hidden state s_t belonging to S, corresponding to a certain observation o_t at time t, and all the hidden states are formed as a hidden state sequence. Matrix $\boldsymbol{A}$ consists of the transition probability between every two hidden states. $a_{i,j}=p(s_{t+1}=j|s_t=i)$, $\forall a_{i,j}\in\boldsymbol{A}$ represents the probability of being a hidden state j at time $t+1$ given that the hidden state equals i at time t ($1\leq t\leq T-1$). If the observation distribution of a given hidden state is discrete, $\boldsymbol{B}$ is the measurement probability matrix. Otherwise, it is a conditional probability distribution function. Taking an example of the discrete case, $b_{i,j}=p(o_t=j|s_t=i)$, $\forall b_{i,j}\in\boldsymbol{B}$ denotes the probability of an observation being j when the hidden state is i at time t ($1\leq t\leq T$). The initial distribution of hidden state π_0 provides the original information without any state transition. Another property of HMM can be expressed as

$$p(s_t\mid o_{t-1},o_{t-2},\ldots,o_1,s_{t-1},s_{t-2},\ldots,s_1)=p(s_t\mid s_{t-1}), \tag{3}$$

$$p(o_t\mid o_{t-1},o_{t-2},\ldots,o_1,s_t,s_{t-1},\ldots,s_1)=p(o_t\mid s_t). \tag{4}$$

This means that the conditional probability distribution of the hidden state at time t depends only on the value of the hidden state at time $t-1$. The values before $t-1$ have no influence on the conditional

distribution. This is called the 'Markov property'. Similarly, the value of the observation at time t depends only on the value of the hidden state s_t.

The modeling object in this study is the velocity vector with three attributes, namely speed, yaw, and pitch. The aircraft performance parameter constraints on the motion state are taken into consideration. This study predicts the velocity attributes at every surveillance update cycle and calculates the next position of the aircraft using a kinematics model. Because of the short update interval, the movement between adjacent instants can be seen as a uniformly accelerating process. In HMM, the hidden state is the motion trend of the aircraft, and the observation is the motion parameter of a different motion trend. The velocity vector at time t can be expressed as

$$\boldsymbol{v}_t = [s_t, \vartheta_t, \theta_t]^{\mathrm{T}}, \tag{5}$$

where s_t, ϑ_t, and θ_t denote the speed, yaw, and pitch of the aircraft in polar coordinates at time t, respectively.

3 Flight model

The estimation of the velocity attributes, i.e., s, ϑ, and θ, is a critical job in trajectory calculation, and the aim of our model is to obtain the velocity of an aircraft at every update moment. The main task is to mine a reasonable description for the parameters of the HMM-based model from the historical flight paths. The observation of the model is the sequence of collected velocity vectors in the trajectory database, and the hidden state is the motion trend of the aircraft. Because of the continuous variation of motion parameters, $\boldsymbol{B}$ in Eq. (2) is a measurement probability distribution function.

3.1 Hidden state set and observation

The hidden state in our model denotes the motion trend of the aircraft. It cannot be directly observed through the saved flight trajectory. HMM solves this issue by computing the relationship between hidden states and observations. Obviously, the observation sequence is the velocity vector in polar coordinates in this model. The hidden state set should be a finite set, and it needs to be manually specified. The goal of this section is to assign the motion states by analyzing the motion patterns.

Because of the uniform accelerating motion process between neighboring points, the motion trend can be classified into three types: constant acceleration (P), constant velocity (C), and constant deceleration (D) (Zheng and Zhou, 2012; Qiao SJ et al., 2015a). The relative orientation between two neighboring positions is determined by the current flight heading. As known, the flight heading gradually and irreversibly changes, and the turn angle must be less than 90° in theory (less than 60° in practice). Therefore, the turn trend has three options: turn left (L), go straight ahead (H), and turn right (R). By the same token, the altitude variation is represented by the pitch, and thus it has three types: climb (B), cruise (U), and descent (V). The final hidden state set of the motion trends has 27 members, each of which corresponding to one combination of speed, yaw, and pitch from 3 speed×3 yaw×3 pitch types. The hidden states are labeled as 1 to 27, corresponding to the indices of the elements in the hidden states transition probability matrix.

The conditional probability distribution $p(v_t|s_t=s)$, $\forall s \in S$ represents the speed probability distribution given a certain motion trend. Obviously, the variation in the aircraft speed, heading, and pitch during the flight are subjected to the constraints of aircraft performance parameters, such as maximum acceleration, turning radius, and climb rate.

3.2 Transition probability matrix

The probability distribution of the hidden state transition between different prediction instants is described by the state transition matrix. The matrix should be learned from the historical discrete position data. Let the speed unit be m/s, and the speed difference between two neighboring prediction time instants be $\Delta v = v_{t+1} - v_t$. $\varsigma_v = \{\varsigma_v | \varsigma_v \in \mathbb{N}^*\}$ is an adaptive parameter to estimate the speed trend. Taking the monitoring device error into consideration, the trend of speed would be estimated by the constant velocity (C) when $-\varsigma_v \le \Delta v \le \varsigma_v$, constant deceleration (D) when $\Delta v < -\varsigma_v$, and constant acceleration (P) when $\Delta v > \varsigma_v$. The yaw and pitch are expressed in degrees. It also requires adaptive parameters ς_ϑ and ς_θ (positive decimal) for estimating the trend of yaw and pitch. These three parameters [ς_v, ς_ϑ, ς_θ] are determined by conducting several experiments. The dimensionality of the transition probability matrix is 27×27 since

there are 27 hidden states in our model.

For example, assume that there is only one transition existing in our model process, and it can be expressed as

$$\boldsymbol{v}_t=[220,10.5,6]^{\mathrm{T}}, \tag{6}$$

$$\boldsymbol{v}_{t+1}=[230,15.9,8]^{\mathrm{T}}. \tag{7}$$

The motion trend sequence is decoded as <PHB, PRB, DHV>, if the adaptive parameter vector [ς_v, ς_ϑ, ς_θ] is [3, 5, 2]. In the hidden state sequence, the first state PHB and last state DHV are additional states of flight departure and arrival, respectively. The hidden state transition probability should be calculated as follows, forming matrix $\boldsymbol{A}$:

$$p(s_{t+1}=\mathrm{PRB}\,|\,s_t=\mathrm{PHB})=0.5, \tag{8}$$

$$p(s_{t+1}=\mathrm{DHV}\,|\,s_t=\mathrm{PRB})=0.5. \tag{9}$$

With the identifier of hidden states, elements of matrix $\boldsymbol{A}$ are all 0 except $a_{4,7}$=0.5 and $a_{7,24}$=0.5.

3.3 Measurement probability distribution

The observations of HMM based models in this study are motion states, i.e., speed, yaw, and pitch. These values can continuously change within the constraints of aircraft performance parameters. Thus, the matrix $\boldsymbol{B}$ of HMM is a conditional probability distribution function. In this study, GMMs are used to indicate the distribution properties of the measurement probability (Qiao SJ et al., 2015a). The model is expressed as

$$p(X\,|\,\psi)=\sum_{i=1}^{k}a_i N(X\,|\,\mu_i,\sigma_i). \tag{10}$$

In Eq. (10), ψ is the unknown parameter of GMM, containing k independent Gaussian components. For the i^{th} ($i\leq k$) component, a_i is the weight of the component in the whole GMM distribution, and μ_i and σ_i are the mean and standard deviations of the Gaussian component, respectively. The sum of all weights must be equal to 1, i.e., $a_1+a_2+\ldots+a_k=1$. The parameters of GMM consist of the following parts in Eq. (11) and (12), in which ψ_i represents the parameters of a single Gaussian component:

$$\psi=\{\psi_1,\psi_2,\ldots,\psi_k\}, \tag{11}$$

$$\psi_i=\langle a_i,\mu_i,\sigma_i\rangle. \tag{12}$$

4 Parameter learning

After creating the flight model, we need to apply the relevant algorithms to learn the unknown parameters (Alligier et al., 2015; Prento et al., 2015) from the historical trajectory set.

4.1 Learning the transition probability matrix

Based on the definition of HMM, the learning steps of the transition probability matrix are introduced as follows:

1. extracting the velocity components from the attributes of collected points of the historical path;

2. generating the hidden states sequence based on the adaptive parameters, adding PHB and DHV at the beginning and end of the sequences, respectively, and obtaining the quantity of the whole hidden states transition;

3. calculating the transition between various hidden states and forming matrix $\boldsymbol{A}$.

4.2 Learning the measurement probability distribution

Based on the model, the velocity component under different moving trends (hidden states) is first extracted from the historical path. Considering the flight profile, we select k=5 in Eq. (10) to describe the motion parameters during different flight stages. Then, an expectation maximization (EM) algorithm is applied to learn the parameters of GMM. The target function of the iterative training for parameter learning is defined as

$$\psi^{(g+1)}=\arg\max\underbrace{\left\{\int_z\log(p(X,Z\,|\,\psi))\,p(Z\,|\,X,\psi^{(g)})\mathrm{d}z\right\}}_{\varphi(\psi,\psi^{(g)})}, \tag{13}$$

where X is a speed sequence with length n, and Z is the introduced hidden states sequence with the same length n. Let

$$p(X,Z|\psi)=\prod_{i=1}^{n}p(x_i,z_i\,|\,\psi)=\prod_{i=1}^{n}\underbrace{p(x_i\,|\,z_i,\psi)}_{N(\mu_{z_i},\sigma_{z_i})}\underbrace{p(z_i\,|\,\psi)}_{a_{z_i}}, \tag{14}$$

$$p(Z \mid X,\psi)=\prod_{i=1}^{n} p(z_i \mid x_i,\psi)=\prod_{i=1}^{n}\frac{a_{z_i}N(\mu_{z_i},\sigma_{z_i})}{a_l N(\mu_l,\sigma_l)}. \quad (15)$$

Then we can obtain the optimal parameters under the EM frame by solving the target function (13):

$$a_l^{(g+1)}=\frac{1}{N}\sum_{i=1}^{N} p(l \mid x_i,\psi^{(g)}) \quad (16)$$

$$\mu_l^{(g+1)}=\frac{\sum_{i=1}^{N} x_i p(l \mid x_i,\psi^{(g)})}{\sum_{i=1}^{N} p(l \mid x_i,\psi^{(g)})} \quad (17)$$

$$\boldsymbol{\sigma}_l^{(g+1)}=\frac{\sum_{i=1}^{N}[x_i-\mu_l^{(i+1)}]^2 p(l \mid x_i,\psi^{(g)})}{\sum_{i=1}^{N} p(l \mid x_i,\psi^{(g)})} \quad (18)$$

$$p\left(l \mid x_i,\psi^{(g)}\right)=\frac{N(x_i \mid \mu_l,\sigma_l)}{\sum_{t=1}^{k} N(x_i \mid \mu_t,\sigma_t)} \quad (19)$$

4.3 Learning the initial distribution of hidden states

Based on the description of the initial distribution of hidden states, we adopt the unbiased estimate of the Gaussian distribution to learn the parameters for the model:

$$u^*=\frac{1}{n}\sum_{i=1}^{n} x_i,\ \delta^*=\frac{1}{n}\sum_{i=1}^{n}(x_i-u^*)^2. \quad (20)$$

5 Prediction of the velocity sequence

Based on the Bayesian theorem (Mahler, 2011), we can obtain

$$p_{t+1|t}(s_{t+1} \mid V^t)=\int p_{t+1|t}(s_{t+1} \mid s)\,p_{t|t}(s \mid V^t)\mathrm{d}s, \quad (21)$$

$$p_{t+1}(v_{t+1} \mid V^t)=\int p_{t+1}(v_{t+1} \mid s)\,p_{t+1|t}(s \mid V^t)\mathrm{d}s. \quad (22)$$

In Eqs. (21) and (22), all the subscripts represent the indices of prediction instants. V^t is the predicted velocity sequence until time t. $p_{t+1|t}$ is the predicted probability distribution at time t+1 given the predicted sequence V^t. In Eq. (21), the first item in the integral is the hidden state transition probability distribution, and the second item is a corrected value after sampling. In Eq. (22), the first item in the integral is the measurement probability distribution, and the second item is estimation from Eq. (21). After completing the prediction of hidden states, a sampling algorithm is applied to obtain the final estimate. MCMC is a classic sampling algorithm for an n-dimensional vector. The working steps are shown as follows:

1. Initializing x_i (i=1, 2, …, n).
2. For t=0, 1, 2, …,

$$x_1^{t+1} \sim p(x_1 \mid x_2^t,x_3^t,\ldots,x_n^t),$$
$$x_2^{t+1} \sim p(x_2 \mid x_1^{t+1},x_3^t,\ldots,x_n^t),$$
$$\vdots$$
$$x_n^{t+1} \sim p(x_n \mid x_1^{t+1},x_2^t,\ldots,x_{n-1}^t).$$

After sampling the velocity vector, the kinematic equation is adopted to calculate the position at every update instant. To reduce the prediction error, a uniform interpolation is used to correct the calculated position during every update cycle (Fig. 2) (Ding et al., 2015). The distance between the predicted and corrected positions is the correction bias.

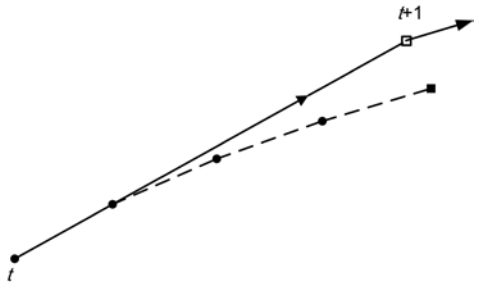

Fig. 2 Corrected position obtained by a uniform interpolation

The hollow and solid square blocks denote the positions predicted and corrected by our method, respectively, at time t

6 Simulation and analysis

In this section, we describe the simulations to verify the adaptive parameters and evaluate the prediction results. The simulation database daily contains the historical paths from January 1, 2015 to

December 30, 2015 for 459 different flights executed. The purpose of our simulation is to predict the plan trajectory on December 30, 2015 for all flights by the historical path from January 1 to December 29, 2015 with the goals of verifying the adaptive parameter and evaluating the prediction results. All the historical paths are preprocessed to keep an identical update cycle. For each flight, let $\mathrm{Tr_c}$ be the collected path in the simulation database, and $\mathrm{Tr_p}$ be the prediction result of our proposed method with the same length (update cycles) of $\mathrm{Tr_c}$ (marked by L). We will introduce the evaluation factors first (Barrios and Motai, 2011; Tang et al., 2016).

1. Prediction error

For $p_t^{\mathrm{c}} \in \mathrm{Tr_c}, p_t^{\mathrm{p}} \in \mathrm{Tr_p}$ $(0 \le t \le L)$, we use the Euclidean distance $d(p_t^{\mathrm{c}}, p_t^{\mathrm{p}})$ to represent the error between the predicted and collected positions:

$$d(p_t^{\mathrm{c}}, p_t^{\mathrm{p}}) = \sqrt{(x_t^{\mathrm{c}} - x_t^{\mathrm{p}})^2 + (y_t^{\mathrm{c}} - y_t^{\mathrm{p}})^2 + (z_t^{\mathrm{c}} - z_t^{\mathrm{p}})^2}. \quad (23)$$

2. Mean and standard deviations of the prediction error

After predicting the trajectory for all 459 flights, the prediction error at every moment for each flight is calculated by Eq. (23). Then the accuracy and stability of the prediction results are depicted by the common statistical characteristics, such as the mean and standard deviations. The mean and standard deviations should be separately computed for a given flight and all flights:

$$\mu_d = \frac{1}{N}\sum_{i=1}^{N} d(p_i^{\mathrm{c}}, p_i^{\mathrm{p}}), \quad (24)$$

$$\delta_d = \sqrt{\frac{1}{N}\sum_{i=1}^{N}\left[d(p_i^{\mathrm{c}}, p_i^{\mathrm{p}}) - \mu_d\right]^2}. \quad (25)$$

6.1 Adaptive modeling parameters

In the modeling process, the choice of different thresholds of speed, yaw, and pitch between two adjacent prediction moments will affect the motion trend estimate. Then the motion pattern distribution will be different, which will further impact the position estimation. Thus, it is important to verify a series of model parameters [ς_v, ς_ϑ, ς_θ] from the historical path using a machine learning algorithm. Several tests are made by varying the parameters within the preset ranges. Pseudo code for tuning adaptive parameters is listed in the Algorithm 1. In this simulation, the evaluation factor is the mean of the prediction error of all 459 flights. It is difficult to visualize the procedure of parameter verification since there are three variables. Therefore, in the visualization process, we fix one parameter ς_v, and then observe the variation in the other two parameters ς_ϑ and ς_θ. Figs. 3–5 show the parameter tuning process. Fig. 3 shows the variation in the prediction error of yaw and pitch when ς_v=12 m/s. Fig. 4 shows the variation in speed and pitch when ς_ϑ=4°. Fig. 5 shows the variation in speed and yaw when ς_θ=6°.

Algorithm 1 Adaptive parameter tuning

Input: range of parameters to be verified
Output: optimal adaptive parameters

```
for speed=S_min to S_max do
  for yaw=Y_min to Y_max do
    for pitch=P_min to P_max do
      Generate the hidden state sequence and group the velocity vectors according to the hidden state.
      Optimize the learnable parameters for GMM.
      Predict the moving trend sequence on the basis of the first state (PHB).
      Sample the motion parameters under different moving trends, and average multiple sampling may be useful for obtaining a stable result.
      Calculate the aircraft positions until landing time and correct positions by a uniform interpolation.
      Measure the prediction error sequence between the collected and predicted values.
      Save the results as mean and standard after computing the mean and standard deviations of the prediction error sequence.
      Compare the result with result_tuple, and assign the smaller one to result_tuple.
    end for
  end for
end for
return result_tuple
```

The following conclusions can be drawn from Figs. 3–5:

1. The mean of the prediction error gradually increases with the increase in adaptive parameters ς_v, ς_ϑ, and ς_θ.

2. In Fig. 3, the mean of the prediction error is not greatly influenced by the difference in pitch (corresponding to the moving trend: climb, cruise,

and descent), but the difference in heading has a stronger effect. The optimal values of pitch and yaw differences are 4° and 6°, respectively.

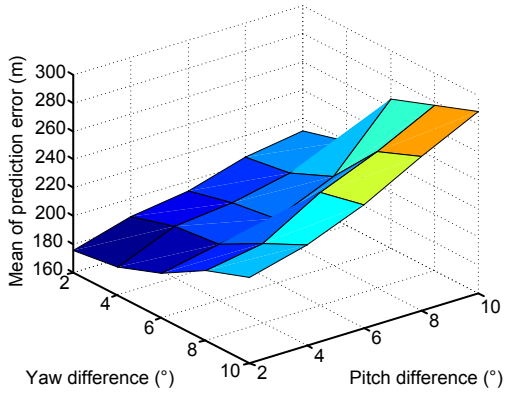

Fig. 3 Diagram of the prediction error with varied yaw and pitch when ς_v=12m/s (References to color refer to the online version of this figure)

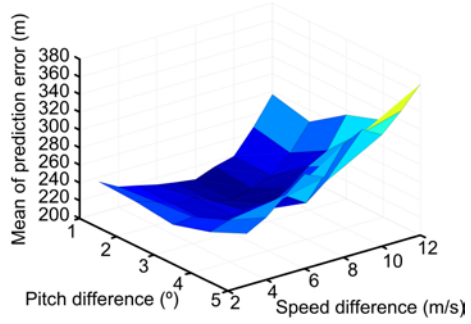

Fig. 4 Diagram of the prediction error with varied speed and pitch when ς_ϑ=4° (References to color refer to the online version of this figure)

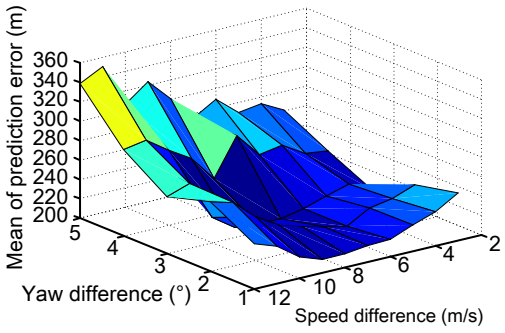

Fig. 5 Diagram of the prediction error with varied speed and yaw when ς_θ=6° (References to color refer to the online version of this figure)

3. In Fig. 4, the mean of the prediction error has a special feature in that the optimal values exist in the bottom of the bowl. The values are neither too large nor too small, but we can clearly see that the prediction error is influenced mainly by the difference in speed (corresponding to the motion trend: acceleration, constant speed, and deceleration). The difference in pitch has a much weaker impact.

4. In Fig. 5, the change in the prediction error is similar to that shown in Fig. 4 except that there is more fluctuation along with the change in the speed difference.

From the above discussions, we know that the variations in speed, yaw, and pitch have different effects on the final prediction result. Therefore, to obtain a more practical result, all these factors should be taken into consideration comprehensively. That is why we model the velocity vector sequence in HMM. The elbow rule, which comes from a machine learning course instructed by Andre Ng, provides good guidance for parameter selection in our simulations. When we encounter a tradeoff between computing complexity and prediction accuracy, we select the maximum parameters before the prediction accuracy deteriorates to reduce the computing complexity. To ensure the accuracy of trajectory prediction, the larger parameters (adaptive parameters) are selected to reduce the computational complexity in the learning and prediction processes.

6.2 Evaluation of the prediction results

Based on the analysis of adaptive parameter tuning in Section 6.1, we determined the parameters for all flights by the simulations, and then processed modeling, learning, and prediction. Once the predicted trajectory is obtained, the comparison with the collected historical trajectory is implemented to evaluate the prediction result. According to the final prediction result, the mean and standard deviations of the prediction error for all 459 flights are about 206.00 and 67.90 m, respectively. The mean and standard deviations of the most accurately forecasted flight are only 79.83 and 39.70 m respectively, while those of the least accurately forecasted flight are up to 535.14 and 176.70 m, respectively. In the visualization phase, it is impractical to put all 459 prediction results on the same graph, so we show our results only for the flight whose prediction error is closest (almost the same) to the overall level. The values of adaptive parameters are listed in Table 1, and the predicted and

collected trajectories are compared in Fig. 6. Fig. 7 shows the prediction error at different update instants. Fig. 8 depicts the prediction error distribution from 0 to 1000 m, where we divided the errors into different levels.

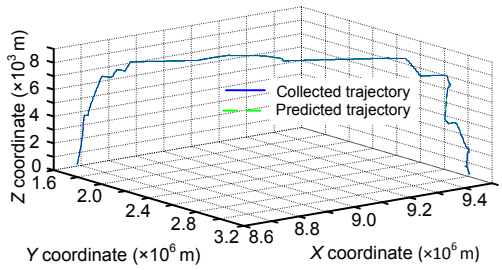

Fig. 6 Comparison between collected and predicted trajectories for a selected flight in the 3D space (References to color refer to the online version of this figure)

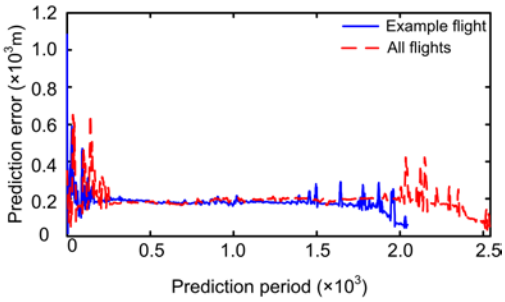

Fig. 7 Comparison of the prediction errors between a selected flight and all flights at different update periods (References to color refer to the online version of this figure)

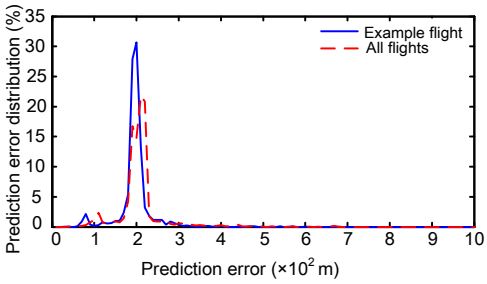

Fig. 8 Comparison of the prediction error distribution between a selected flight and all flights in different ranges (References to color refer to the online version of this figure)

The whole collected and predicted trajectories from the departure to arrival are shown in Fig. 6. For greater contrast, the prediction errors of both the selected example flight and of all flights are shown in Figs. 7 and 8. The prediction errors of both the selected flight and all sampled flights fluctuated in a wider range during the climb and descent stages than that in the cruise stage (Fig. 7). This is the temporal pattern of prediction error distribution. Similarly, the spatial distribution rules can be summarized from Fig. 8, where we can see that most prediction errors occur at around 200 m. Moreover, according to the analysis, we find that the altitude error contributes more during the climb and descent stages, while the horizontal error maintains a relatively high level during the cruise stage.

Table 1 Adaptive parameters for the selected flight

Parameter	Value
ς_v	12 m/s
ς_ϑ	4°
ς_θ	6°

To further prove the superiority of our proposed model, we conduct several simulations to compare our model with other models, including a traditional kinematics and dynamics based model (KDM), a statistical model (HMM) on the flight phase and velocity vector (HMPV), and a GMM based model on position and speed (GMPS). These simulations are conducted on the same dataset and the overall (for all 459 flights) mean and standard deviations of the prediction error are regarded as the evaluation criterion. The results are listed in Table 2. It is clear that our model gives more accurate and stable prediction results than the other methods. As for the traditional KDM method, both the mean and standard deviation are the highest among the listed models because of its simple aerodynamic equations and improper parameter setting. HMPV uses HMM to model the flight phase (climb, cruise, and descent), and kernel functions are applied to describe the law of velocity, so the mean of the prediction error is relatively low (about 361 m). As for GMPS, a GMM is used to model the whole velocity distribution. It is a coarse model which does not consider the discriminative features in different flight environments, but it is also better than KDM due to the learning process. We believe that our algorithm achieves the best performance, because it applies more reasonable and distinctive modeling of the motion parameters.

Table 2 Results of comparative tests

Model	Mean (m)	Standard deviation (m)
KDM	683.55	423.00
HMPV	361.67	168.43
GMPS	406.17	136.58
Our approach	206.35	90.70

7 Conclusions

To meet the urgent demand for accurate trajectory prediction in ATFM systems, we have proposed a hybrid double stochastic statistical model to depict the flying process. A more accurate and credible trajectory prediction has been obtained by calculating the motion equations with a predicted velocity sequence. The main idea of this work is that the motion trend has high similarity for the same route and the dynamic parameters of aircraft can be described by a learnable distribution. Taking the implicit uncertainties into consideration, the proposed model focuses mainly on mining the motion characteristics from historical trajectories during the flight by modeling the 3D velocity vector. In accordance with the basic idea, a double stochastic process is designed using HMM and GMM to model the motion trend and parameters, respectively. Machine learning algorithms are applied to optimize the learnable parameters for the models and distributions. The hidden state sequence is predicted by selecting the highest probability from the proposed model, and MCMC is then used to sample the dynamic motion parameters from the measurement probability distribution. The aircraft position sequence is calculated using a kinematic equation, and a correctiion procedure is achieved by interpolation. Simulations are conducted to verify the modeling parameters and estimate the trajectories for all flights. By comparison with the collected ground truth data, the validity of our method is proved by evaluating the prediction errors. The results of further comparative tests show that our proposed algorithm achieves more accurate and stable results. Therefore, our proposed model may be an excellent solution for trajectory prediction in ATM and simulation systems.

Two extensions to this method are possible: more efficient algorithms can be developed to learn the parameters and predict the trajectory; an overall prediction for the whole air traffic situation would provide a better solution to the problems when facing the civil aviation industry. We will continue our research along these two directions.

References

Alligier R, Gianazza D, Durand N, 2015. Machine learning and mass estimation method for ground-based aircraft climb prediction. *IEEE Trans Intell Transp Syst*, 16(6): 3138-3149. https://doi.org/10.1109/TITS.2015.2437452

Ayhan S, Samet H, 2016. Aircraft trajectory prediction made easy with predictive analytics. ACM SIGKDD Int Conf on Knowledge Discovery & Data Mining, p.21-30.

Barrios C, Motai Y, 2011. Improving estimation of vehicle's trajectory using the latest global positioning system with Kalman filtering. *IEEE Trans Instrum Meas*, 60(12): 3747-3755. https://doi.org/10.1109/TIM.2011.2147670

Chen ZJ, 2010. Theory and Method of Airspace Management. Science Press, Beijing, China, p.217-227 (in Chinese).

Ding ZM, Yang B, Güting RH, et al., 2015. Network-matched trajectory-based moving-object database: models and applications. *IEEE Trans Intell Transp Syst*, 16(4): 1918-1928. https://doi.org/10.1109/TITS.2014.2383494

Gardi A, Sabatini R, Ramasamy S, et al., 2013. 4-Dimensional trajectory negotiation and validation system for the next generation air traffic management. AIAA Guidance, Navigation, and Control Conf, p.1-15.

Hamed MG, Gianazza D, Serrurier M, et al., 2013. Statistical prediction of aircraft trajectory: regression methods vs point-mass model. 10th USA/Europe Air Traffic Management Research and Development Seminar, p.1-11.

Jeung HY, Shen HT, Zhou XF, 2007. Mining trajectory patterns using hidden Markov models. Int Conf on Data Warehousing and Knowledge Discovery, p.470-480.

Li Z, Li SH, Wu XL, 2015. General aircraft 4D flight trajectory prediction method based on data fusion. Int Conf on Machine Learning and Cybernetics, p.309-315.

Lymperopoulos I, Lygeros J, 2010. Sequential Monte Carlo methods for multi-aircraft trajectory prediction in air traffic management. *Int J Adapt Contr Signal Process*, 24(10):830-849. https://doi.org/10.1002/acs.1174

Mahler PSR, 2011. Statistical Multisource-Multitarget Information Fusion. National Defense Industry Press, Beijing, China, p.27-37 (in Chinese).

Morzy M, 2007. Mining frequent trajectories of moving objects for location prediction. Proc 5th Int Conf on Machine Learning and Data Mining in Pattern Recognition, p.667-680.

Naseri A, Neogi N, Rantanen E, 2007. Stockastic hybrid models with applications to air traffic management. AIAA Guidance, Navigation, and Control Conf and Exhibit, p.370-379.

Prento T, Thom A, Blunck H, et al., 2015. Making sense of

trajectory data in indoor spaces. IEEE Int Conf on Mobile Data Management, p.9424-9436.

Qiao MY, Bian W, Xu RYD, et al., 2015. Diversified hidden Markov models for sequential labeling. *IEEE Trans Knowl Data Eng*, 27(11):2947-2960. https://doi.org/10.1109/TKDE.2015.2433262

Qiao SJ, Jin K, Han N, et al., 2015a. Trajectory prediction algorithm based on Gaussian mixture model. *J Softw*, 26(5):1048-1063.

Qiao SJ, Shen DY, Wang XT, et al., 2015b. A self-adaptive parameter selection trajectory prediction approach via hidden Markov models. *IEEE Trans Intell Transp Syst*, 16(1):284-296. https://doi.org/10.1109/TITS.2014.2331758

Shanmuganathan SK, 2014. A HMM-Based Prediction Model for Spatio-Temporal Trajectories. MS Thesis, the University of Texas at Arlington, Dallas, USA.

Song LL, 2012. A 4-D trajectory prediction method based on set of historical trajectory. *Comput Technol Dev*, 12:11-14.

Tang KS, Zhu SF, Xu YQ, et al., 2016. Modeling drivers' dynamic decision-making behavior during the phase transition period: an analytical approach based on hidden Markov model theory. *IEEE Trans Intell Transp Syst*, 17(1):206-214. https://doi.org/10.1109/TITS.2015.2462738

Tang XM, Chen P, Zhang Y, 2015a. 4D trajectory estimation based on nominal flight profile extraction and airway meteorological forecast revision. *Aerosp Sci Technol*, 45:387-397. https://doi.org/10.1016/j.ast.2015.06.001

Tang XM, Gu JW, Shen ZY, et al., 2015b. A flight profile clustering method combining TWED with *K*-means algorithm for 4D trajectory prediction. Integrated Communication, Navigation, and Surveillance Conf, p.1-9.

Tang XM, Zhou L, Shen ZY, et al., 2015c. 4D trajectory prediction of aircraft taxiing based on fitting velocity profile. 15th COTA Int Conf of Transportation Professionals, p.1-12.

Wandelt S, Sun XQ, 2015. Efficient compression of 4D-trajectory data in air traffic management. *IEEE Trans Intell Transp Syst*, 16(2):844-853.

Xie AM, Cheng P, 2015. 4D approaching trajectory design in terminal area based on radar data. *Appl Mech Mater*, 740:731-735. https://doi.org/10.4028/www.scientific.net/AMM.740.731

Yepes JL, Hwang I, Rotea M, 2007. New algorithms for aircraft intent inference and trajectory prediction. *J Guid Contr Dynam*, 30(2):370-382. https://doi.org/10.2514/1.26750

Zahariand A, Jaafar J, 2015. Combining hidden Markov model and case based reasoning for time series forecasting. *Commun Comput Inform Sci*, 513:237-247. https://doi.org/10.1007/978-3-319-17530-0_17

Zhang JF, Jiang HX, Wu XG, 2014. 4D trajectory prediction based on BADA and aircraft intent. *J Southwest Jiaotong Univ*, 49(3):553-558.

Zheng Y, Zhou XF, 2012. Computing with Spatial Trajectories. Springer, New York, USA, p.337-394.